Determination of Cross-Link Density in Thermoset Polymers by Use of Solid-State ^1H NMR Techniques

Charles G. Fry and Arthur C. Lind*

McDonnell Douglas Research Laboratories, St. Louis, Missouri 63166.
Received June 1, 1987

ABSTRACT: Solid-state ^1H NMR techniques were used to determine the cross-link density of highly cross-linked polymers common in the aerospace industry. As the temperature was increased, the spin–spin relaxation times of cross-linked epoxy polymers were observed to reach a plateau value which increased linearly with increasing molecular weight between cross-links, as predicted by theory. The results show that, for the epoxy system studied, approximately 10 rotatable backbone bonds are needed to form a statistical segment, the portion of the polymer backbone that moves independently of the other backbone motions.

Introduction

The macroscopic properties of a thermoset polymer, such as hardness, impact strength, brittleness, and elasticity, are intrinsically related to the molecular motions occurring within the cured thermoset; therefore, it is important to quantify the dependence of these motions on the cross-link density. Theoretical studies of the effects of cross-links and entanglements on motions within a polymer are extensively documented.[1] Experimental studies, however, have dealt primarily with lightly cross-linked materials. The results of a preliminary ^1H NMR study[2,3] of highly cross-linked epoxy polymers suggested the validity of a theory[4] that relates the spin–spin relaxation time to the cross-link density. This paper presents the results of a more complete ^1H NMR study which provide an agreement with the theory for highly cross-linked epoxy resin systems of importance to the aerospace industry.

An important quantity used to investigate motions of a polymeric chain is the average squared direction cosine of the angle between some vector rigidly attached to the chain and a fixed direction determined by the experiment. Nuclear magnetic resonance (NMR) is a sensitive technique for investigating $\langle \cos^2 \theta \rangle$, where θ is the angle between a particular proton–proton vector (or C–D bond vector for deuterium NMR) and the static magnetic field direction. The hydrogen dipole–dipole interactions are usually the dominant interactions in solids, and they therefore determine the hydrogen spin–spin relaxation time, T_2, of such systems. When a polymer is heated above the glass transition temperature, T_g, extensive molecular motion occurs at a rate faster than T_2^{-1}, thus an increase in T_2 is observed when the hydrogen dipole–dipole interactions are averaged by the molecular motions. Heating increases molecular motion until the constraints of the cross-links at each end of the chain prevent further averaging. As a result, the measured T_2 increases with increasing temperature to a plateau whose value, T_2^p, is a function of the cross-link density. The smaller the cross-link density, ρ_c, the greater is the allowed number of orientations for an average chain. Thus, reducing ρ_c increases T_2^p. For lightly cross-linked materials, the quantity T_2^p has been shown to be inversely proportional to ρ_c:[4]

$$T_2^p \propto \rho_c^{-1} \tag{1}$$

In our study we relate $\langle \cos^2 \theta \rangle$ to T_2^p, determined in an epoxy resin system by NMR, and show that the relationship in eq 1, and also more sophisticated analyses, holds for this highly cross-linked system.

Experimental Section

We have studied a series of epoxy resins having different cross-link densities. The cross-link densities were varied by curing the epoxy, the diglycidyl ether of bisphenol A (DGEBA), with different amounts of the amines, *N,N'*-dimethyl-1,6-diaminohexane (DDH) and 1,4-diaminobutane (DAB) (see Figure 1). Samples of DGEBA were room-temperature cured by careful mixing with stoichiometric amounts of six different mixtures of the tetrafunctional amine DAB and the difunctional amine DDH. The samples were placed into 5-mm-diameter NMR tubes, evacuated, and sealed under ~100 torr of N_2. Postcuring was performed during the NMR experiments at elevated temperatures.

The samples are denoted as *X*:*Y*:*Z* where *X* refers to the equivalents of DAB, *Y* refers to the equivalents of DDH, and *Z* refers to the equivalents of DGEBA used in the mixture. In these experiments, all samples were made from stoichiometric mixtures of amines and epoxy, so that $X + Y = Z$. The DAB:DDH:DGEBA ratios studied were 0:5:5, 1:4:5, 2:3:5, 3:2:5, 4:1:5, and 5:0:5. Because of the functionalities of the amines, the 5:0:5 sample had the largest cross-link density.

The pulsed ^1H NMR measurements were performed on an in-house-designed, single-coil spectrometer operating at 100 MHz. An external fluorine lock sample at 94 MHz was used to control the magnet (Varian V-4014) so that small signals could be signal averaged for long times without the attendant drift (with locking, the drift was <100 Hz/h). The 100- and 94-MHz rf signals were derived from a frequency synthesizer (Hewlett-Packard HP5100), and the 8-mT-pulsed rf magnetic field was generated with a programmable digital pulser and a 100-W linear amplifier (Electronic Navigation Industries 3100L). The dead time of the receiver/probe circuit was <7 μs. A transient recorder (Nicolet 4094) was used to acquire and store the signals, and either a DEC PRO-380 or a VAX-780 computer was used for the analyses.

Data were obtained for each sample at 11 temperatures in the range 300–530 K. The temperature was controlled by passing dry air over a heating coil located close to the probe and monitoring the temperature at the air inlet and outlet of the probe with copper–constantan thermocouples. The inlet thermocouple was connected directly to an Omega Model 6002-TR temperature controller, which held the setpoint inlet temperature to <±0.1 K. By disconnecting the rf transmitter from the probe and inserting a thermocouple directly into the rf coil, we found the actual sample temperature to be controlled to better than ±2 K.

T_2^p was found by computer fitting each ^1H NMR decay signal. The fitting routine, FCDA (five-component decay analysis), is built around a generalized fitting procedure called ZXSSQ, copyrighted by IMSL.[5] FCDA allows the user to define up to five component decays to be included in the fit, along with a base-line parameter. The form of the fitted equation is then

$$S(t) = a_1 \exp[-(t/T_{2_1})^{n_1}] + \ldots + a_5 \exp[-(t/T_{2_5})^{n_5}] + C \tag{2}$$

where the parameters a_j, T_{2_j}, and n_j are the fractional amplitude, spin–spin relaxation time, and line-shape parameter, respectively, for the *j*th component decay, and *C* is the base-line parameter. Each parameter can be fixed or fitted, depending on the user's input. The user can choose decays to be Lorentzian, $n_j = 1$, Gaussian, $n_j = 2$, or other, n_j = (user defined or fitted) in character. The fits extrapolate the experimental data back to time $t = 0$, assumed to occur at the midpoint of the initial rf pulse.

Both the experiments and the fitting procedures had to be varied according to the time regimes of the T_2 values observed for a particular sample at a particular temperature. Fitting the

0024-9297/88/2221-1292$01.50/0

Resin:

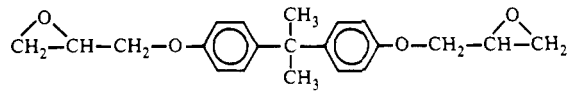

DGEBA

Curing agents:

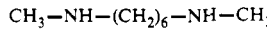

DDH

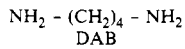

DAB

Figure 1. Curing agents and the epoxy resin used in this study.

Table I
Data Analysis Procedures for Epoxy Resin Experiments

T_{2f}, μs	NMR experiment	line-shape assumptions
<40	FID	Gaussian (fast) + Lorentzian (slow)
<200	FID	Lorentzian (fast) +
	CPMG	Lorentzian (slow)
>200	FID and CPMG	Lorentzian (fast) + Lorentzian (slow)

relaxation decays with two components assumed to be either two Lorentzians or a Gaussian and a Lorentzian always produced fits within 4% of the initial magnetization (see the discussion of difference spectra below). Equation 2 thus becomes

$$S(t) = a_f \exp[-(t/T_{2f})^{n_f}] + a_s \exp(-t/T_{2s}) + C \qquad (3)$$

where f stands for fast decay and s for slow decay, and $n_f = 1$ or 2.

The experimental and fitting procedures used for determining T_2^P are listed in Table I. The T_{2f} component arises from the entangled or cross-linked polymer, whereas the T_{2s} component is most likely due to the more mobile chain ends which are not tied down.[6] Since the plateau region of interest here is due to the entangled or cross-linked polymer, we are primarily concerned with measuring T_{2f} as a function of ρ_c and temperature. Thus, to be more specific, we will denote the plateau value obtained as T_{2f}^P. Since T_{2s} is not used in this study, we need not be concerned with its line-shape character. Free-induction decays[7] (FID) were measured at all temperatures to monitor the fast-decaying component. The Carr–Purcell–Meiboom–Gill (CPMG) spin–echo pulse sequence[8] was used to determine decay times longer than 200 μs. The CPMG technique eliminated broadening caused by magnet inhomogeneity (~65 Hz) and chemical shift dispersion (~700 Hz). Various echo times were used and were always long enough to ensure that spin-locking of the magnetization during the CPMG sequence would not occur.

Difference spectra generated by subtracting the fitted data from the raw data were used to check the validity of each fit. Typical results from the fitting procedure are shown in Figure 2. The largest errors in a particular fit always occurred near the beginning of the fit. We fit decays using more than two components in many ways but found that eq 3 always produced fits that were within 4% of the initial intensity. To keep the analyses as straightforward as possible, we present here only the results obtained by use of eq 3.

Theory

Gotlib et al.[4] developed a theoretical treatment relating ^{1}H NMR spin–spin relaxation times to cross-link densities and showed experimental evidence that suggested the theory might apply to lightly cross-linked systems. The basic equation in Gotlib et al.'s treatment is the following:[9,10]

$$\overline{\cos^2 \gamma} = \left(1 - \frac{2h}{zb\beta}\right) = \frac{1}{3} + \frac{2}{5}\left(\frac{h}{zb}\right)^2 + \frac{24}{175}\left(\frac{h}{zb}\right)^4 + \ldots \qquad (4)$$

where γ defines the angle between the vector connecting a specific proton pair of interest to the vector connecting the cross-link points (as shown in Figure 3), z is the number of freely jointed statistical segments of length b between cross-links, h is the distance between cross-link points, and $\beta = L^{-1}(h/zb)$, L^{-1} being the inverse Langevin function. Equation 4 is based on the concepts of freely jointed chains as described in the work of Kuhn and Grün.[10] For lightly cross-linked systems, $h \ll zb$, and the average squared distance between cross-links $\bar{h}^2 = zb^2$ ($\bar{h} \equiv$ mean h) so that

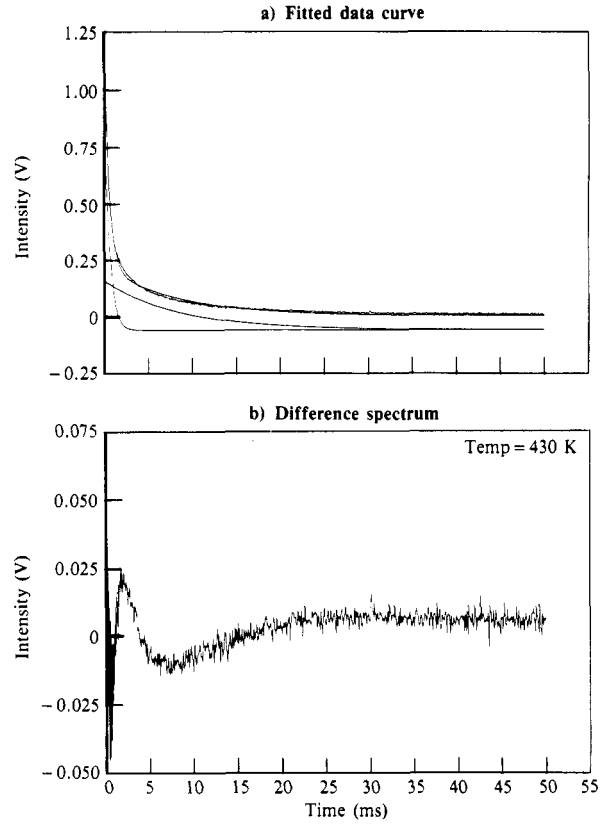

Figure 2. Typical curve fitting results and difference spectra. (a) A Lorentzian + Lorentzian fit to CPMG data obtained from the 1:4:5 sample at 430 K. The fit runs through the raw data, whereas the two component curves are displaced downward for clarity. (b) This difference curve is the raw data minus the fitted curve shown in (a).

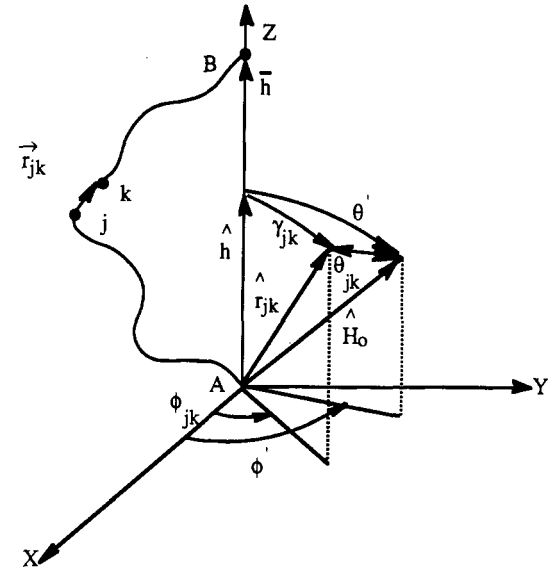

Figure 3. Coordinates in the molecular frame. Points A and B are the cross-link points. h is the cross-link distance. The vector $\vec{r}_{jk}$ extends from the jth to the kth atom in the chain. $\hat{H}_0$ is the unit vector parallel to the laboratory static magnetic field direction. $\hat{r}_{jk}$ is the unit vector parallel to $\vec{r}_{jk}$.

$$3\overline{\cos^2\gamma} - 1 \simeq 6/5z \quad (5)$$

For highly cross-linked systems, however, Gotlib et al.'s formulation is based on the persistent chain model[11] wherein (eq 7 in ref 4 is incorrect)

$$3\overline{\cos^2\gamma} - 1 = 2[15x - 26 + (9x + 27)\exp(-x) - \exp(-3x)][x - 1 + \exp(-x)]/\left[15x^3 - 52x^2 - 18x(4 + x)\exp(-x) + \frac{2}{3}x\exp(-3x) + (214/3)x\right] \quad (6)$$

The quantity x is the ratio of the contour length to the persistence length, which equals $5z/3$ for $x \rightarrow \infty$ (note also that the right-hand side of eq 6 approaches 2 for $x \rightarrow 0$, and $2/x$ as $x \rightarrow \infty$).

There are a number of serious assumptions involved in the derivations of eq 4–6 which become more important as ρ_c gets larger. The most serious of these is the freely jointed chain approximation. For highly cross-linked systems, all current analytical methods contain varying levels of assumptions. Numerical methods are available which include restricted chain motions caused by molecular interactions and we will present the results of such an investigation in a future paper.

Other approximations must be made when relating eq 5 and 6 to the NMR spin–spin relaxation times. The second moment of a rigid-lattice line shape, M_2, is usually written as[12]

$$M_2 = \frac{3}{2N}\gamma_m{}^4h^2I(I+1)\sum_{j<k}\frac{(3\cos^2\theta_{jk} - 1)^2}{r_{jk}{}^6} \quad (7)$$

where N is the number of spins, I is the spin quantum number, γ_m is the magnetogyric ratio, and r_{jk} is the distance from spin j to spin k. Motion is introduced by assuming that the major changes in the second moment will be in $\theta_{jk} = \theta_{jk}(t)$; i.e., the angle between the protons changes significantly with time while the spacing between nearest neighbors stays essentially the same. This latter assumption is strictly true only for nuclei bonded to the same atom.

Now we transform $\theta_{jk}(t)$ into the molecular frame. Dropping the subscripts jk for legibility we have

$$\tfrac{1}{2}(3\cos^2\theta - 1) = P_2(\cos\theta) = \frac{4\pi}{5}\sum_{m=-2}^{2} Y_2{}^{m*}(\gamma,\phi)Y_2{}^m(\theta',\phi') \quad (8)$$

where γ,ϕ are the spherical angles of $\vec{r}_{jk}$ in the molecular frame and θ',ϕ' are the spherical angles of the static field vector in the molecular frame as shown in Figure 3. P_2 is the Legendre polynomial and $Y_2{}^m$ are the spherical harmonics. The square of $(3\cos^2\theta_{jk} - 1)$ must be used for static, powder averaging (i.e., averaging over conformations varying in times $\gg T_2$).

If we assume that the chain moves isotropically with respect to ϕ in a time $\ll T_2$, eq 8 becomes

$$\langle(3\cos^2\theta_{jk} - 1)\rangle_\phi = \tfrac{1}{2}(3\cos^2\theta' - 1)(3\cos^2\gamma_{jk} - 1) \quad (9)$$

Equation 9 is applicable when the internuclear vector connecting the two protons is parallel to the chain segment axis, as shown in Figure 3. If instead the internuclear vector of the two interacting protons makes a fixed angle δ_{ij} with respect to the chain segment axis, and these protons are free to rotate in a cone of half-angle δ_{ij} about the chain segment axis in a time short compared to T_2, then eq 9 is replaced by

$$\langle(3\cos^2\theta_{ij} - 1)\rangle_\phi = \tfrac{1}{4}(3\cos^2\theta' - 1)(3\cos^2\delta_{ij} - 1)(3\cos^2\gamma_{ij} - 1) \quad (10)$$

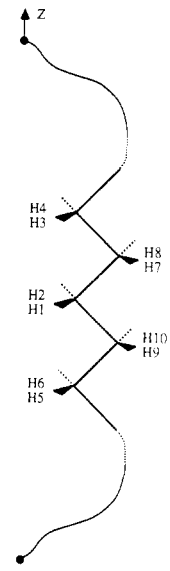

Figure 4. Exploded view of a section of a polyethylene chain. Interproton distances and angles are listed in Table II.

Assuming that cross-links are isotropically distributed throughout the sample gives $\overline{(3\cos^2\theta' - 1)^2} = {}^4/_5$ and by separation of the sum in eq 7 into the static distance dependence and the time-varying θ components, the rigid lattice second moment is

$$M_2{}^{RL} = \frac{3}{10N}\gamma_m{}^4h^2I(I+1)\sum_{j<k}r_{jk}{}^{-6} \quad (11)$$

and the second moment is then approximately

$$M_2 = \tfrac{1}{16}M_2{}^{RL}\langle(3\cos^2\delta - 1)^2\rangle(3\overline{\cos^2\gamma} - 1)^2 \quad (12)$$

where the δ term is an approximate value (see below). The last term in eq 12 can now be substituted by either eq 5 or 6. Note that the average is over $\cos^2\gamma$ only for a time-averaged process. To get an expression in T_2, we use the second moment expression for a Lorentzian line shape with 2% cutoffs[12] for systems undergoing motions[13]

$$M_2 = 2(46)^{1/2}/\pi T_2{}^2 \quad (13)$$

and the second moment expression for a Gaussian line shape for rigid systems

$$M_2{}^{RL} = (T_2{}^{RL})^{-2} \quad (14)$$

Rather than calculating $M_2{}^{RL}$ from eq 11, we use the experimentally measured $T_2{}^{RL}$; thus, combining eq 12–14, we obtain

$$T_2 = 8.3T_2{}^{RL}|\langle(3\cos^2\delta - 1)^2\rangle^{1/2}(3\overline{\cos^2\gamma} - 1)|^{-1} \quad (15)$$

Substitution with eq 5 yields

$$T_2 = 6.9T_2{}^{RL}z\langle(3\cos^2\delta - 1)^2\rangle^{-1/2} \quad (16)$$

The last term in eq 16 deserves attention. Since δ is different for different proton pairs in the polymer chain, the evaluation of $\langle(3\cos^2\delta - 1)^2\rangle^{-1/2}$ is not straightforward. δ for the diaminoalkanes used in this study can be estimated by considering a section of polyethylene chain, as shown in Figure 4. The interaction pairs H1–H3 and H1–H5 are, on average, parallel to the segment axis, so $\delta_{13} = 0$ and $(3\cos^2\delta_{13} - 1)^2 = 4$. The interaction pair H1–H2, the strongest of all the pairs is, on the other hand, on average perpendicular to the segment axis, and $(3\cos^2\delta_{12} - 1)^2 = 1$. Other important interaction pairs and their

Table II
Polyethylene Model Used To Estimate $\langle(3\cos^2\delta - 1)^2\rangle^{-1/2}$

proton pair ik	r_{ik}, nm	δ_{ik}	$1/r_{ik}^6$, nm^{-6}	$(3\cos^2\delta_{ik} - 1)^2/r_{ik}^6$, nm^{-6}
H1–H2	0.180	90°	29600	29600
H1–H3,5	0.254	0°, 180°	3725	14900
H1–H4,6	0.313	35°, 145°	1065	1025
H1–H7,9	0.252	60°, 120°	3905	245
H1–H8,10	0.310	66°, 114°	1125	285
			$\sum_{k=2}^{10} = 49240$	62510

contributions are listed in Table II, from which an average δ can be defined according to

$$\langle(3\cos^2\delta - 1)^2\rangle\sum_k \frac{1}{r_{ik}^6} \sim \sum_k \frac{(3\cos^2\delta_{ik} - 1)^2}{r_{ik}^6} \quad (17)$$

From eq 17 and the results for polyethylene chains in Table II, $\langle(3\cos^2\delta - 1)^2\rangle^{-1/2} \sim 0.9$ for the diaminoalkanes used in this study. A similar analysis on DGEBA yields the same approximate value, and we therefore use

$$\langle(3\cos^2\delta - 1)^2\rangle^{-1/2} \sim 0.9 \quad (18)$$

Equation 18 is a "best guess". The reader should be aware of the large uncertainty arising from the approximation given in eq 18 (e.g., $\langle(3\cos^2\delta - 1)^2\rangle^{-1/2} \to \infty$ for a system where all $\delta_{jk} = 54.7°$). Inserting eq 18 into eq 16 gives

$$T_2 = 6.2T_2^{RL}z \quad (19)$$

We have presented a detailed derivation of eq 19 to emphasize some of the more important assumptions made along the way. We consider the following to be most important. First, the time dependence of r_{jk} in proton studies would seem to be nonnegligible, and use of eq 7 should be considered for a more accurate analysis. The use of eq 8 may become necessary for systems having strong interchain interactions or other interactions which constrain the chain motions in such a way that the averaging of ϕ in eq 9 or rotation about the chain segment axis in eq 10 becomes invalid. The assumptions made in eq 5 and 6 concerning constraints on the chain motions appear to be inappropriate for the epoxy resins systems studied here; however, they will both be shown to be adequate for relating T_{2f}^p to the cross-link density. Finally, the assumptions about the NMR line shape made in eq 13 and the estimation of $\langle(3\cos^2\delta - 1)^2\rangle^{-1/2}$ in eq 18 may limit the accuracy obtainable for some results.

In terms of predicting the behavior of the NMR spin–spin relaxation time, T_{2f}, however, we will show that the above assumptions combined to derive eq 19 adequately describe the epoxy resin system used in this study. This description is realized by use of an adjustable parameter, the number of rotatable bonds per statistical segment. If no adjustable parameters are permitted in the analysis, a numerical solution could be obtained by evaluating the average of eq 7 over all the allowed chain conformations, taking into account the specific details of the molecular structure of the polymer chain and the constraints produced by the cross-link points.

Results and Discussion

The values of T_{2f} obtained by use of FCDA for each epoxy sample at each temperature are plotted in Figure 5. The plateau area is observed at ~60 °C above T_g for all but the 0:5:5 sample, which theoretically has no cross-links. (In practice, ether cross-links form by competing reactions.)

T_g can be estimated from the data presented in Figure 5 as the point of intersection of the relatively flat low-temperature region to the slope of the sudden increase in T_{2f}. Values found in this way agree within experimental

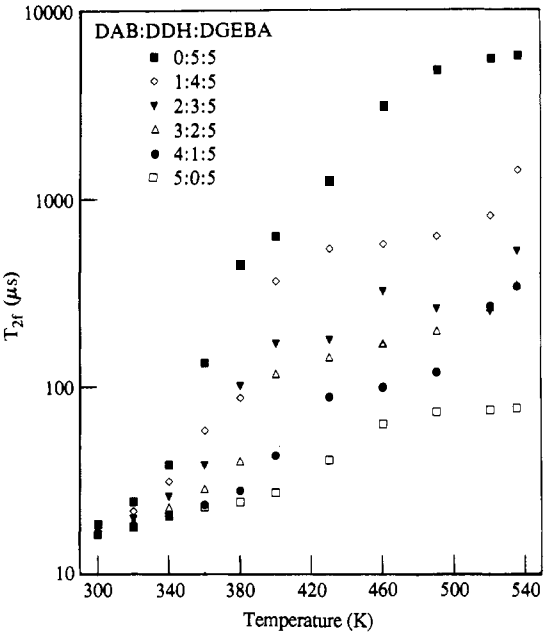

Figure 5. T_{2f} values obtained for each sample for the preselected 11 temperatures.

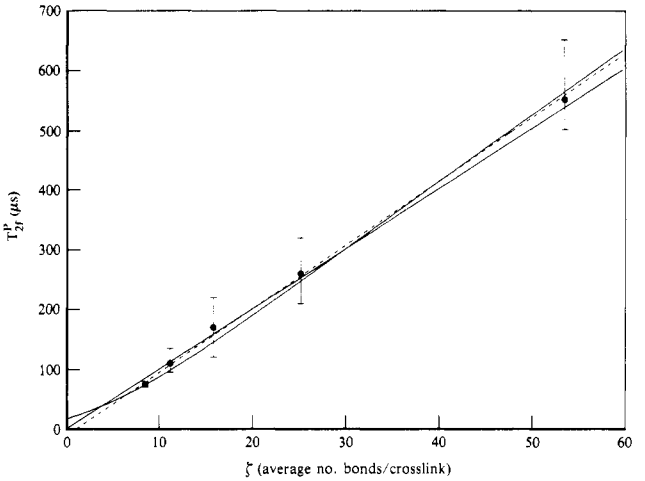

Figure 6. Weighted least-squares fits of eq 19 and 25 to the T_{2f}^p values obtained from the data in Figure 5. The curved line is the fit to eq 25 with the intercept equaling 17.0 μs, and $\zeta = 0.17x$. The straight line through zero is the fit to eq 19 having a slope equaling 10.0, whereas the dashed line has an intercept of −11.4 μs and slope of 10.5.

Table III
Glass Transition Temperatures, T_g, Determined by NMR and Dynamic Mechanical Analyses

	T_g, K	
sample	NMR, from T_{2f}[a]	dynamic mechanical, tan δ
0:5:5	330	329
1:4:5	343	
2:3:5	355	348
3:2:5	372	364
4:1:5	388	
5:0:5	405	408

[a] This measurement is accurate to ±10 K.

error with T_g's determined by dynamic mechanical measurements on similarly prepared samples[2] as shown in Table III.

The region where T_{2f} = 200–500 μs was problematic during the analyses. This region not only lies within the T_2 regime where chemical shift dispersion begins to affect

the FID (it introduces a beat due to the chemical shift between the aliphatic and the aromatic protons) but is also where the analysis of the CPMG data is least accurate due to the small number of data points obtainable for reasonable echo times. The large error bars given in Figure 6 reflect this experimental limitation.

Above 520 K the samples experience some degradation, and this degradation is reflected in the data in this temperature regime. For example, a large crack was observed in the 5:0:5 sample following the 520 K run, and the 4:1:5 sample turned slightly brown during the 530 K run. Values of T_{2f}^{P} were obtained, therefore, from the data below 520 K.

The molecular weight between cross-links, M_c, is calculated from the composition in the following way. The average molecular weight per equivalent in a sample having an $X:Y:Z$ composition is

$$\bar{M} = \left(\frac{X}{4}M_x + \frac{Y}{2}M_y + \frac{Z}{2}M_z\right)(X + Y + Z)^{-1} \quad (20)$$

where M_x (=88) is the molecular weight of the tetrafunctional DAB, M_y (=144) is the molecular weight of the difunctional DDH, and M_z (=340) is the molecular weight of the difunctional DGEBA. The DAB molecule is treated as two trifunctional cross-link points connected by *n*-butane. (DAB contains two cross-link points per 4 equiv.) Hence the number of trifunctional cross-link points per equivalent is given by

$$\rho_e = 2\frac{X}{4}(X + Y + Z)^{-1} \quad (21)$$

In general, a polymer that has *n*-functional cross-link points has *n* chains connecting every two cross-link points. Therefore, in this case where $n = 3$, the average molecular weight per chain between cross-links is given by

$$\bar{M}_c = \frac{2}{3}\frac{\bar{M}}{\rho_e} = \frac{\frac{X}{4}M_x + \frac{Y}{2}M_y + \frac{Z}{2}M_z}{3\frac{X}{4}} \quad (22)$$

The average number of rotatable backbone bonds per chain between cross-link points, ζ, is estimated by assuming that DAB has five, DDH has seven, and DGEBA has ten such backbone bonds. Thus,

$$\zeta = \frac{2}{3}\frac{5\frac{X}{4} + 7\frac{Y}{2} + 10\frac{Z}{2}}{\rho_e(X + Y + Z)} = \frac{5\frac{X}{4} + 7\frac{Y}{2} + 10\frac{Z}{2}}{3\frac{X}{4}} \quad (23)$$

We are interested in ζ because of its (as yet, undetermined) relationship to z, the number of freely jointed statistical segments per chain between cross-links. Values for M_c and ζ derived by use of eq 22 and 23 are listed in Table IV.

The experimentally determined T_{2f}^{P} values plotted as a function of ζ are shown in Figure 6. T_{2f}^{P} varies linearly with ζ (and M_c) within experimental error, as predicted by eq 5, except for the value for the 5:0:5 sample. This slope equals 10.0 ± 0.5 μs. For very highly cross-linked samples (ζ and $M_c \rightarrow 0$), the linear behavior must break down since T_{2f}^{P} must approach not zero, but instead a rigid lattice limit usually found to be 15–20 μs (see eq 11 and 14); Figure 5 shows $T_2^{RL} = 17 \pm 1$ μs for the DAB/DDH/DGEBA epoxy systems. Since the limiting behavior does not give zero, as implied by eq 5, a linear fit including an intercept is shown as the dashed line in Figure 6, and now all the T_{2f}^{P} values fall very close to the line. The slope of this fit is 10.5 ± 0.3 μs. Inserting the slope and T_2^{RL} values into eq 19, we calculate that $\zeta = (10 \pm 1)z$; i.e., 10 rotatable bonds in this system approximate a freely jointed statistical segment. The error bar given above results only from the goodness-of-fit of the data in Figure 6. Other possible errors, especially those from eqs 13 and 18, lead us to give a more conservative estimate

$$\zeta = (10 \pm 3)z \quad (24)$$

Table IV
Calculated Cross-Link Parameters for the DAB/DDH/DGEBA Samples

sample DAB/DDH/DGEBA	av molecular wt btwn cross-links, M_c, g	av no. of rotatable bonds btwn cross-links, ζ
0:5:5	∞	∞
1:4:5	1547	53.7
2:3:5	740	25.3
3:2:5	471	15.9
4:1:5	337	11.2
5:0:5	256	8.3

The more extensive theoretical treatment described by eq 6 is also plotted in Figure 6, where the correct intercept is clearly shown. The equation plotted in Figure 6 is

$$T_2 = 0.9\{4 + 4.3[1 - \exp(-\zeta/10)]\}T_2^{RL}\Omega(c\zeta \rightarrow x) \quad (25)$$

where $\Omega(c\zeta \rightarrow x)$ is equal to the inverse of the right side of eq 6 with $c\zeta$ substituted for x, c being a proportionality constant. This equation was fit to the data to determine T_2^{RL} and c. The expression in the brackets of this equation is a mathematical artifice used to produce the correct limiting values for T_2 in the rigid and motionally averaged regions (see the discussion associated with eq 13 and 14). As shown in Table I, the fast decaying NMR signal was approximately Gaussian for $T_{2f} < 40$ μs and it was approximately Lorentzian for $T_{2f} > 200$ μs. Figure 6 shows that $\zeta = 5$ when $T_{2f} = 40$ μs, and $\zeta = 20$ when $T_{2f} = 200$ μs. Therefore, the expression in the brackets was chosen to go from 4 for a Gaussian to 8.3 for a Lorentzian, with the major change occurring in the region $5 < \zeta < 20$. The fit of eq 25 to the data yielded $T_2^{RL} = 17$ μs, in agreement with the measured value, and $c = 0.17$. Equation 25 was also fit by using a constant value of 8.4 in the brackets because most of the data is in the Lorentzian region; c was still equal to 0.17, but T_2^{RL} was incorrectly determined to be 36 μs. Thus, the expression in the brackets of eq 25, while not rigorous, is a useful artifice for satisfying both the Gaussian and Lorentzian conditions. The significant result of these fits to the data is that $c = 0.17$, because this (along with $x = c\zeta$ and $x = 5z/3$ for large x) leads to the conclusion that $\zeta = 10z$, in agreement with eq 24 which was obtained by using eq 5.

Equation 24 implies that approximately 10 rotatable backbone bonds undergo correlated motions independent of similar units along the polymer backbone. In terms of averaging NMR spin–spin relaxation times, basic aspects of the freely jointed chain theory[10] hold true even for highly cross-linked epoxy resins. For the most highly cross-linked systems (for $z \sim 1$), it appears that the freely jointed view of a statistical segment revolving about each cross-linked end much like a rigid rod turning about its C_∞ axis provides an adequate description. We have obtained preliminary molecular modeling results that, at least qualitatively, confirm this assertion.

An understanding of the dependence of eq 24 on the molecular weight per rotatable backbone bone (for these epoxies, this is ~30), of the chemical functionality along the backbone, and of side chains and chain packing would enable us to better understand the impact of these microscopic features on the macroscopic mechanical and physical properties of polymers.

Conclusions

We find that the current theoretical description of motions in cross-linked polymers[4] is applicable to highly cross-linked epoxy resin systems, at least for determining the cross-link density of a material of unknown composition. We also find that ^1H NMR spin–spin relaxation times plateau above T_g in epoxy thermoset resins, and the plateau values increase linearly with the average number of bonds between cross-links, even in the most highly cross-linked systems. For the epoxy system we studied, approximately 10 backbone bonds are necessary to define a statistical segment, a portion of a chain which moves independently of the rest of the chain motions.

Acknowledgment. This research was conducted in part under Naval Air Systems Command Contract N00019-80-C-0552 and in part under the McDonnell Douglas Independent Research and Development program. We are grateful to Jeff Huber for his assistance in acquiring and analyzing much of the data presented in this paper.

Registry No. (DGEBA)(DDH)(DAB) (copolymer), 99037-53-3; (DGEBA)(DDH) (copolymer), 31832-83-4; (DGEBA)(DAB) (copolymer), 69777-26-0.

References and Notes

(1) Flory, J. *Statistical Mechanics of Chain Molecules*; Interscience: New York, 1969.
(2) Brown, I. M.; Lind, A. C.; Sandreczki, T. C. *Magnetic Resonance Determinations of Structure and Reaction Kinetics of Epoxy/Amine Systems*, Technical Report MDC Q0759 (Dec 31, 1981, Naval Air Systems Command Contract N00019-80-C-0552.
(3) Lind, A. C. *Bull. Am. Phys. Soc.* **1983**, *28*, 433.
(4) Gotlib, Yu. Ya.; Lifshits, M. I.; Shevelev, V. A.; Lishanskii, I. S.; Balanina, I. V. *Polym. Sci. USSR (Engl. Transl.)* **1976**, *18*, 2630.
(5) ZXSSQ and complimentary subroutines are copyrighted by IMSL, Inc., NBC Building, Houston, TX 77036-5085.
(6) For example: Charlesby, A.; Bridges, B. J. *Eur. Polym. J.* **1981**, *17*, 645–656.
(7) For example: Farrar, T. C.; Becker, E. D. *Pulse and Fourier Transform NMR*; Academic: New York, 1971; Chapter 2.
(8) Meiboom, S.; Gill, D. *Rev. Sci. Instrum.* **1958**, *29*, 688.
(9) Reference 4 contains some errors (as pointed out in the text) and a confusing figure (we reproduce it as Figure 3) and glosses over some important points. For these reasons, we reproduce and expand the theory introduced in ref 4.
(10) Kuhn, W.; Grün, F. *Kolloid-Z.* **1942**, *101*, 248.
(11) Gotlib, Yu. Ya. *Polym. Sci. USSR (Engl. Transl.)* **1964**, *6*, 429.
(12) Abragam, A. *The Principles of Nuclear Magnetism*; Oxford University Press: Oxford, 1961; Chapter IV.
(13) The factor of $46^{1/2}$ in eq 12 would be replaced by $\pi/2$ for a Gaussian line shape and replaced by $99^{1/2}$ for 1% cutoffs for a Lorentzian line shape.

Vibrational Spectra and Structure of Polyaniline

Y. Furukawa, F. Ueda, Y. Hyodo,† and I. Harada*

Pharmaceutical Institute, Tohoku University, Aobayama, Sendai 980, Japan

T. Nakajima and T. Kawagoe

Technical Research Laboratory, Bridgestone Corporation, 3-1-1, Ogawahigashi-cho, Kodaira-shi, Tokyo 187, Japan. *Received September 3, 1987*

ABSTRACT: Vibrational spectra have been studied on polyaniline in various forms with different electrical properties: two conducting forms, as-polymerized (2S) and doped 1A polyanilines; and three insulating forms, reduced-alkali-treated (1A), acid-treated 1A (1S), and oxygen-treated 1A [1A(O_2)] polyanilines. Polyaniline 1A is spectroscopically evidenced to be poly(imino-1,4-phenylene), —(NHC_6H_4)$_n$—. Polyaniline 1S consists of imino-1,4-phenylene (IP) unit (—NHC_6H_4—) and its salt unit (—$NH_2^+A^-$—C_6H_4—, (A^-, anion)). Treatment of 1A with oxygen converts part of consecutive IP units (—$NHC_6H_4NHC_6H_4$—) to nitrilo-2,5-cyclohexadiene-1,4-diylidenenitrilo-1,4-phenylene (NP) unit (—N=C_6H_4=NC_6H_4—). Semiquinone radical cations of IP units exist only in the conducting forms of polyaniline, 2S and doped 1A, indicating that semiquinone radical cations play an important role in electrical conduction in polyaniline.

Introduction

Polyaniline is an interesting material because it is not only an electrically conducting polymer[1-8] but also a good material as an electrode of a secondary battery with aqueous or nonaqueous electrolytes.[9-15] Polyaniline polymerized from aniline in aqueous acid solution is converted to several forms with different electrical properties by acid/base treatments and oxidation/reduction (see Figure 1). The as-polymerized form (2S[16]) gives high electrical conductivity (~5 S/cm).[1-7] It becomes insulating when treated with aqueous alkaline solution[2-6] (2A) or reduced electrochemically in aqueous acid solution (1S).[7] Reduced-alkali-treated polyaniline (1A) also is insulating[4,8] and it is unstable in air; its color changes from white to blue upon exposure to air. Polyaniline 1A doped with electrolyte anions[14] (doped 1A) is obtained by electrochemical oxidation and it was found, in this work, to be a new conducting form (σ = 5.8 S/cm). Recently, a secondary lithium battery with a 1A pellet (as the cathode) and nonaqueous electrolytes has been developed as a power source of memory back up and a maintenance-free power source combined with a solar battery.[9,13]

It is important to elucidate the structure of each form of polyaniline for understanding its properties. In a preceding paper[17] Furukawa et al. studied the Raman and infrared spectra of as-polymerized (2S) and alkali-treated (2A) polyanilines and electrochemical reduction process from 2S to 1S using some structural key bands. It was shown that the 2A form is a hybrid of the imino-1,4-phenylene (IP) unit (—NHC_6H_4—) and nitrilo-2,5-cyclohexadiene-1,4-diylidenenitrilo-1,4-phenylene (NP) unit (—N=C_6H_4=NC_6H_4—) containing quinone diimine structure (—N=C_6H_4=N—) and that high electrical conductivity in the 2S form is due to the presence of

† Present address: Eli Lilly Japan K. K., Kobe Kanden Building, 2-1, Kano-cho, 6-Chome, Chuo-ku, Kobe 650, Japan.

0024-9297/88/2221-1297$01.50/0